doi:10.1016/j.jmb.2012.04.022 J. Mol. Biol. (2012) 420, 284–295

Contents lists available at www.sciencedirect.com

Journal of Molecular Biology

journal homepage: http://ees.elsevier.com.jmb

Plasmodium falciparum SSB Tetramer Binds Single-Stranded DNA Only in a Fully Wrapped Mode

Edwin Antony†, Alexander G. Kozlov†, Binh Nguyen and Timothy M. Lohman*

Department of Biochemistry and Molecular Biophysics, Washington University School of Medicine, 660 South Euclid Avenue, Box 8231, St. Louis, MO 63110-1093, USA

Received 11 January 2012; received in revised form 16 March 2012; accepted 6 April 2012
Available online 26 April 2012

Edited by S. Kowalczykowski

Keywords:
DNA repair; recombination; replication; structure; malaria

The tetrameric *Escherichia coli* single-stranded DNA (ssDNA) binding protein (*Ec*-SSB) functions in DNA metabolism by binding to ssDNA and interacting directly with numerous DNA repair and replication proteins. *Ec*-SSB tetramers can bind ssDNA in multiple DNA binding modes that differ in the extent of ssDNA wrapping. Here, we show that the structurally similar SSB protein from the malarial parasite *Plasmodium falciparum* (*Pf*-SSB) also binds tightly to ssDNA but does not display the same number of ssDNA binding modes as *Ec*-SSB, binding ssDNA exclusively in fully wrapped complexes with site sizes of 52–65 nt/tetramer. *Pf*-SSB does not transition to the more cooperative $(SSB)_{35}$ DNA binding mode observed for *Ec*-SSB. Consistent with this, *Pf*-SSB tetramers also do not display the dramatic intra-tetramer negative cooperativity for binding of a second $(dT)_{35}$ molecule that is evident in *Ec*-SSB. These findings highlight variations in the DNA binding properties of these two highly conserved homotetrameric SSB proteins, and these differences might be tailored to suit their specific functions in the cell.

Introduction

Malaria is the one of the deadliest diseases in human history and still accounts for millions of deaths annually.[1] *Plasmodium falciparum*, the causative parasite for malaria, is a member of the apicocomplexan genus and is defined by the presence of a unique plastid-like organelle called the apicoplast. The apicoplast is a vital organelle for the survival of the parasite and is the site of isoprenoid synthesis.[2] It contains its own 35-kb genome that encodes for a variety of metabolic proteins, but not proteins involved in DNA metabolism, which are synthesized in the nucleus and targeted to the apicoplast.[3]

The single-stranded DNA (ssDNA) binding protein of *P. falciparum* (*Pf*-SSB) is one such protein that is believed to play a role in the maintenance of the apicoplast genome.[4] The *Escherichia coli* SSB (*Ec*-SSB) protein is essential for cell survival, and small molecules that interfere with its function are being developed as potential antibiotics.[5,6] By analogy, the *Pf*-SSB protein might also serve as a novel target for the development of antimalarial compounds.

SSB proteins bind tightly to ssDNA during DNA replication and repair. The homotetrameric *Ec*-SSB is a well-characterized bacterial SSB protein and the prototype for many biochemical, structural, and mechanistic analyses.[7–12] *Pf*-SSB shares a high degree of sequence and structural similarity with

*Corresponding author. E-mail address: lohman@biochem.wustl.edu.

† E.A. and A.G.K. contributed equally to this work.

Abbreviations used: SSB, single-stranded DNA binding protein; ssDNA, single-stranded DNA; *Pf*-SSB, *Plasmodium falciparum* SSB; *Ec*-SSB, *Escherichia coli* SSB; FRET, fluorescence resonance energy transfer; smFRET, single-molecule fluorescence resonance energy transfer; ITC, isothermal titration calorimetry; HMM, hidden Markov model; mtSSB, mitochondrial SSB protein.

Ec-SSB[4] (E.A. *et al.*, accompanying article). Both proteins are homotetramers with each subunit containing two domains, an OB-fold that forms the ssDNA binding site and an unstructured C-terminus. A key difference between the two proteins is at the extreme end of the C-termini. *Ec*-SSB contains a nine-amino-acid acidic sequence (MDFDDDIPF) that binds to more than a dozen proteins that function in DNA replication, repair, and recombination.[8] In *Pf*-SSB, this C-terminal region is replaced by KMNVQEFEE. This raises the likely possibility that *Pf*-SSB also binds to a set of interacting partners that are specific to function(s) in the apicoplast.

The binding of *Ec*-SSB to ssDNA has been well studied and is complex due to the fact that the tetramer possesses four potential ssDNA binding sites.[8,9] The *Ec*-SSB tetramer is able to bind ssDNA in multiple binding modes, referred to as $(SSB)_N$, where "N" can be 35, 55, or 65, and denotes the number of nucleotides occluded by a single tetramer.[13–16] The transition among the different modes can be modulated *in vitro* by protein-to-DNA binding density,[17,18] as well as salt concentration and type, with multivalent cations being more effective.[13–16] At high salt concentrations, the $(SSB)_{65}$ mode, in which all four subunits of the tetramer interact with ssDNA that wraps fully around the tetramer occluding ~65 nt, is favored. At lower salt concentrations and high SSB-to-ssDNA ratios, the $(SSB)_{35}$ mode, in which an average of only two subunits of the tetramer interact with the ssDNA, is favored. In the $(SSB)_{35}$ binding mode, SSB tetramers can bind to a long ssDNA with positive inter-tetramer cooperativity to form long protein clusters.[9,16] A third mode, $(SSB)_{55}$, has also been observed in binding to poly(dT), although this mode has not been well characterized.[13]

Crystal structures of the tetrameric DNA binding core of *Ec*-SSB bound to ssDNA have shown the topology of ssDNA wrapping in the $(SSB)_{65}$ mode and suggested a model for the partial ssDNA wrapping in the $(SSB)_{35}$ mode.[19] *Ec*-SSB tetramers bind short ssDNA fragments with an intra-tetramer negative cooperativity such that the first two subunits bind with higher affinity than the remaining two subunits.[20–22] This negative cooperativity increases with decreasing salt concentration and plays a role in promoting the $(SSB)_{35}$ binding mode on longer ssDNA. The precise functions of these various DNA binding modes are still not clear, but SSB in its $(SSB)_{65}$ binding mode has been shown to promote the formation of RecA nucleoprotein filaments on ssDNA by transiently melting DNA secondary structures such as hairpins ahead of filament formation.[10,18] The ability of an SSB tetramer to diffuse along ssDNA without dissociating is critical for this function.[10,11] The observed formation of cooperative SSB protein clusters along ssDNA in its $(SSB)_{35}$ binding mode suggests that this mode of binding might function in DNA replication.[7,16]

In an accompanying article (E.A. *et al.*), we describe a crystal structure of the DNA binding core of the *Pf*-SSB tetramer bound to two molecules of $(dT)_{35}$ in a fully wrapped $(SSB)_{65}$-like mode. Here, we compare the ssDNA binding properties of the *Pf*-SSB and *Ec*-SSB proteins. We find that the *Pf*-SSB tetramer can bind ssDNA in a fully wrapped complex with occluded site sizes ranging from 55 to 62 nt on poly(dT), reminiscent of the $(SSB)_{55}$ and $(SSB)_{65}$ binding modes of *Ec*-SSB.

Surprisingly, we find no evidence that *Pf*-SSB tetramers can form the highly cooperative $(SSB)_{35}$ binding mode even at low [NaCl] that favors this mode for *Ec*-SSB. Consistent with this observation, *Pf*-SSB does not display the dramatic intra-tetramer negative cooperativity for binding short ssDNA molecules that is a hallmark of *Ec*-SSB.[20–22] These observations suggest that the $(SSB)_{35}$ mode may not be used by *Pf*-SSB in its functions in the apicoplast.

Results

Occluded binding site size of *Pf*-SSB tetramers on poly(dT)

One of the primary parameters describing the nonspecific binding of a protein to a long, polymeric DNA is its occluded site size, defined as the number of DNA nucleotides that the protein occludes in its complex with DNA.[23] Note that the occluded site size is not necessarily the same as the number of nucleotides that contact the protein.

In the case of the *Ec*-SSB tetramer, the occluded site size is dependent upon the salt concentration and type with both anion and cation effects.[13,15,17] On poly(dT) at 25 °C, *Ec*-SSB shows well-defined modes of binding ssDNA with occluded site size of 65 ± 3 and 55 ± 3 nt/tetramer at high salt down to ~35 ± 3 nt/tetramer at low salt.[13]

In an accompanying article (E.A. *et al.*), we have shown that *Pf*-SSB is also a stable tetramer that can wrap ssDNA; hence, we examined its occluded site size and determined whether this also changes with [NaCl]. We measured the occluded site size on poly(dT) by monitoring the associated quenching of *Pf*-SSB tryptophan fluorescence upon binding poly(dT) in buffer H (25 °C) as a function of [NaCl] (4 mM to 1 M). Just as is the case with *Ec*-SSB, *Pf*-SSB binds to poly(dT) stoichiometrically under all [NaCl] examined, and representative titrations performed at 4 mM NaCl and 200 mM NaCl are shown in Fig. 1a and b, respectively, yielding site sizes of 50 ± 2 and 58 ± 2 nt/tetramer, respectively. Similar titrations were performed over a range of [NaCl], and the measured occluded site

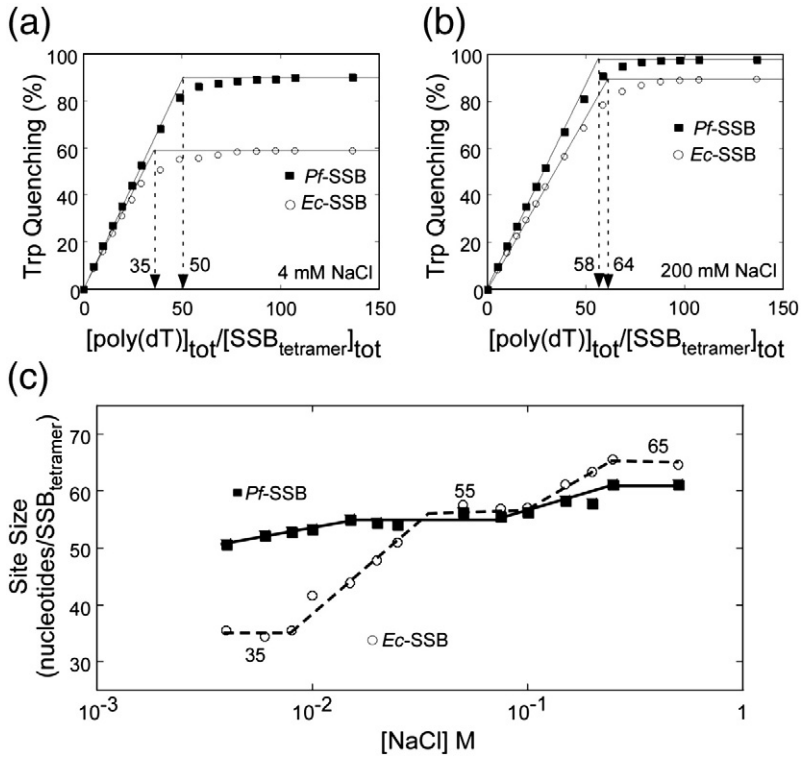

Fig. 1. Determination of occluded site size of SSB on poly(dT) DNA. (a) Representative fluorescence titrations of *Pf*-SSB and *Ec*-SSB with poly(dT) in buffer H with 4 mM NaCl (a) or 200 mM NaCl (b), respectively. The occluded site size was determined from the intersection of the two straight lines as indicated and is 35 and 50 nt at 4 mM NaCl and 65 and 58 nt at 200 mM NaCl for *Ec*-SSB and *Pf*-SSB, respectively. (c) [NaCl] dependence of the change in occluded site size of *Pf*-SSB and *Ec*-SSB. The lines denote a transition between a low salt binding mode (*Pf*-SSB = 50 nt and *Ec*-SSB = 35 nt) and a high salt binding mode (*Pf*-SSB = 60 nt and *Ec*-SSB = 65 nt). Both proteins also appear to have an intermediate binding mode around 55 nt.

sizes are plotted *versus* [NaCl] in Fig. 1c. The occluded site sizes for *Pf*-SSB range from 50 ± 2 to 62 ± 2 nt/tetramer, with plateau values of 62 ± 2 above 200 mM NaCl and a plateau value of 55 ± 4 nt/tetramer from 80 to 100 mM NaCl. Below 20 mM NaCl, there is a slight decrease in site size from 55 to ~50 nt/tetramer. Titrations performed at several *Pf*-SSB concentrations (0.2–0.6 μM) gave the same results at each [NaCl] (data not shown). For comparison, Fig. 1c also shows the occluded site sizes measured for the *Ec*-SSB tetramer under the same conditions. These occluded site sizes measured for *Ec*-SSB and the effects of [NaCl] agree well with previously measured values.[13,15] Both the *Pf*-SSB and *Ec*-SSB tetramers show well-defined plateau regions with site sizes of ~55 and 62–65 nt/tetramer indicating stable $(SSB)_{55}$ and $(SSB)_{65}$ binding modes on poly(dT). However, surprisingly, the *Pf*-SSB tetramer does not show evidence for a stable low site size $(SSB)_{35}$ mode that clearly forms with *Ec*-SSB below 10 mM NaCl. This indicates a clear difference between *Ec*-SSB and *Pf*-SSB binding to ssDNA.

The amplitude of the Trp fluorescence quenching upon binding poly(dT) also reflects the extent of wrapping of ssDNA around the SSB tetramer.[13,15] In the case of *Ec*-SSB bound to poly(dT), the $(SSB)_{35}$ binding mode shows a ~50–60% fluorescence quenching, reflecting the fact that, on average, only two subunits interact with poly(dT) in this mode (Fig. 1a), whereas in the $(SSB)_{65}$ binding mode, ~90% fluorescence quenching is observed since all four subunits interact with poly(dT) in this mode (Fig. 1b).[15] For *Pf*-SSB, we observe 88–92% Trp fluorescence quenching at low [NaCl] (0–50 mM NaCl, Fig. 1a) and a 96–98% quenching at higher [NaCl] (Fig. 1b), suggesting that all four subunits contact the poly(dT) at all [NaCl]. These results suggest that *Pf*-SSB tetramer forms a fully wrapped complex with poly(dT) at all [NaCl] and does not transition to a lower site size $(SSB)_{35}$ binding mode, in stark contrast to *Ec*-SSB.

Pf-SSB does not display unlimited cooperative DNA binding

At low salt concentrations and high SSB-to-DNA binding densities, *Ec*-SSB tetramers can bind in a low site size $(SSB)_{35}$ binding mode that displays an unlimited inter-tetramer positive cooperativity in its binding to long ssDNA.[15,16,18] This mode of binding results in the formation of protein clusters on the ssDNA as demonstrated by the formation of SSB filaments on long M13mp18 ssDNA using electron microscopy.[18] Binding of *Ec*-SSB to M13 ssDNA has been shown to decrease the contour length of DNA in both its $(SSB)_{65}$ and $(SSB)_{35}$ modes but to different extents due to the different degrees of ssDNA wrapping around the tetramer.[14,18] Examples of electron microscopy pictures of *Ec*-SSB tetramers bound to M13 circular ssDNA are shown in Fig. 2c (low [NaCl]) and Fig. 2d (high [NaCl] and Fig. S1). At low salt concentrations and high protein binding density, *Ec*-SSB forms filaments on ssDNA with an extended contour length (Fig. 2c) compared to

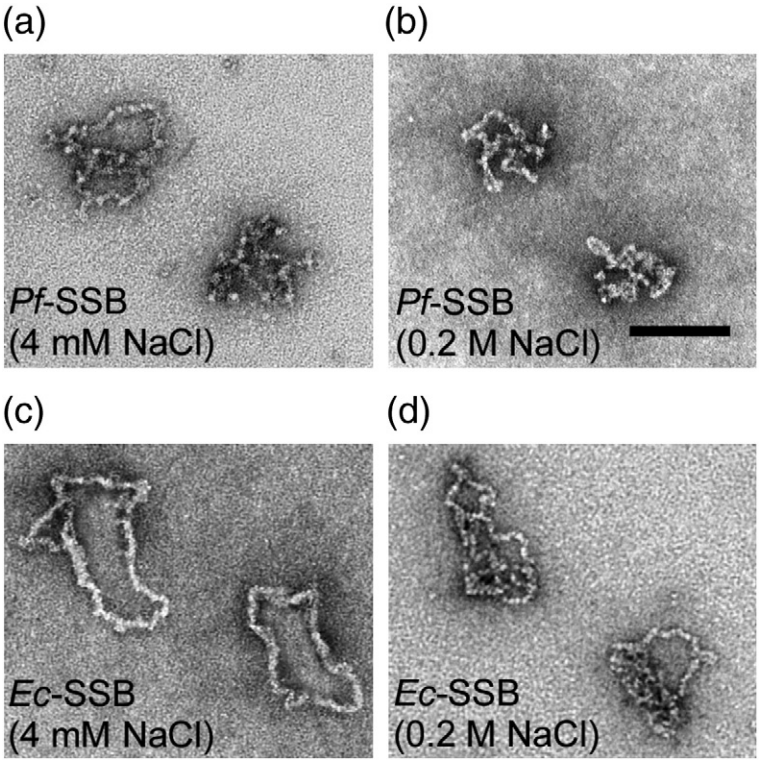

Fig. 2. Electron microscopy images of *Ec*-SSB or *Pf*-SSB bound to M13mp18 ssDNA. On M13ssDNA, *Pf*-SSB forms only the punctate, collapsed, fully wrapped SSB–DNA complexes at both low [4 mM, (a)] and moderate [200 mM, (b)] [NaCl], suggestive of the $(SSB)_{65}$ binding mode. Larger, cooperative, unlimited SSB–DNA filaments are observed with *Ec*-SSB in low [4 mM, (c)] NaCl conditions, suggesting the presence of the $(SSB)_{35}$ binding mode. *Ec*-SSB at moderate [NaCl] [200 mM, (d)] forms punctate, collapsed, fully wrapped SSB–DNA complexes reflecting formation of the $(SSB)_{65}$ binding mode.

smaller, nucleosome-like structures with much smaller contour lengths that are formed at higher [NaCl] (Fig. 2d).[14,18] In contrast, *Pf*-SSB binding to M13 circular ssDNA displays only the more compact nucleosome-like structures at both low and high [NaCl] at all protein binding densities (Fig. 2a and b). We see no evidence of a highly cooperative binding mode. These results are consistent with the fluorescence titrations and the occluded site size measurements and suggest that *Pf*-SSB does not form a partially wrapped $(SSB)_{35}$ binding mode (as shown schematically in Fig. 3a).

The transition of the *Ec*-SSB tetramer from the $(SSB)_{65}$ mode to the $(SSB)_{35}$ mode has also been monitored on a $(dT)_{68}$ molecule labeled on one end with a Cy3 fluorophore and on the other end with a Cy5 fluorophore.[24,25] This fluorophore pair can undergo fluorescence resonance energy transfer (FRET) from the Cy3 donor to the Cy5 acceptor. When one *Ec*-SSB tetramer is bound to this ssDNA in the fully wrapped $(SSB)_{65}$ mode, the Cy3 and Cy5 fluorophores are in very close proximity and thus display high FRET. However, when two *Ec*-SSB tetramers are bound in the $(SSB)_{35}$ mode, the FRET is reduced (Fig. 3a). Therefore, the change in Cy5 fluorescence due to FRET can be used to monitor both *Ec*-SSB binding and the transition from the $(SSB)_{65}$ to the $(SSB)_{35}$ binding mode.[25]

As shown in Fig. 3b, upon initial titration of the Cy3-$(dT)_{68}$-Cy5 with either *Ec*-SSB or *Pf*-SSB (buffer H, pH 8.1, 80 mM NaCl, 25 °C), a high FRET (high Cy5 fluorescence) complex is formed with 1:1 stoichiometry, consistent with formation of a 1:1 fully wrapped $(SSB)_{65}$ complex. Upon further titration with *Ec*-SSB, a decrease in Cy5 fluorescence is observed, reflecting the binding of a second *Ec*-SSB tetramer to the DNA, resulting in a further separation of the Cy3 donor and Cy5 acceptor fluorophores (Fig. 3b). In contrast, after the initial formation of a 1:1 *Pf*-SSB–Cy3-$(dT)_{68}$-Cy5 complex, very little decrease in Cy5 fluorescence is observed upon further addition of *Pf*-SSB. Even at a 15-fold molar excess of *Pf*-SSB tetramer, a second *Pf*-SSB tetramer does not bind to the DNA (Fig. 3b). This behavior also suggests that the *Pf*-SSB tetramer is not able to form the $(SSB)_{35}$ binding mode under these conditions.

Pf-SSB tetramers bind two molecules of $(dT)_{35}$ with high affinity but little intra-tetramer negative cooperativity

At saturation, an *Ec*-SSB tetramer can bind two molecules of $(dT)_{35}$. The first $(dT)_{35}$ molecule binds with high affinity, whereas the second $(dT)_{35}$ binds with much weaker affinity, indicative of negative cooperativity that becomes more extreme as the [NaCl] is reduced.[20–27] The salt-dependent change in negative cooperativity correlates closely with the salt-dependent transition between *Ec*-SSB binding modes formed on poly(dT).[7,20,21] We therefore examined whether *Pf*-SSB displays a salt-dependent negative cooperativity in its binding of $(dT)_{35}$.

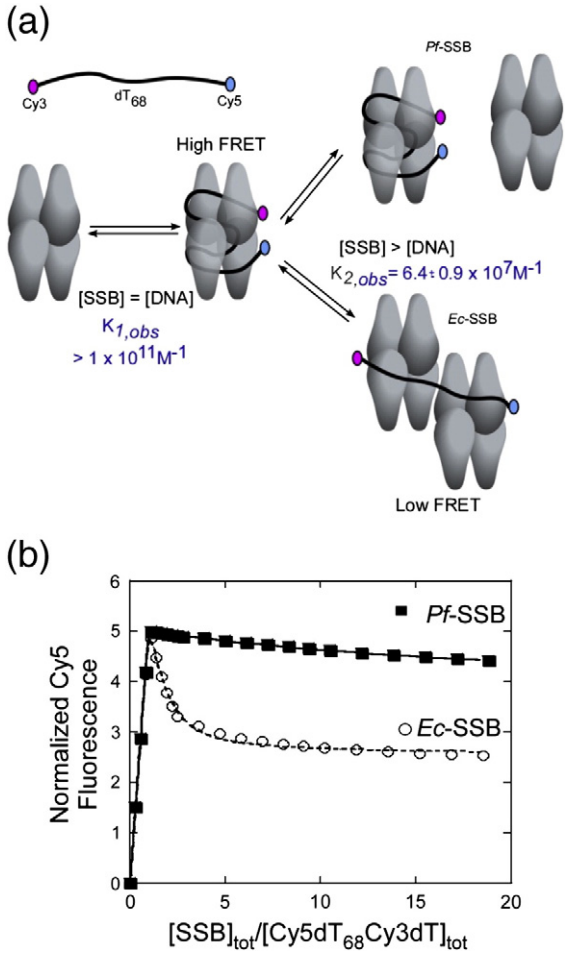

Fig. 3. Multiple DNA binding modes are observed for *Ec*-SSB, but not for *Pf*-SSB. *Pf*-SSB or *Ec*-SSB concentration-dependent changes in DNA binding modes. Results of an equilibrium titration of 5′-Cy5-dT_{68}-Cy3-T-3′ (0.1 μM) with SSB (in buffer H + 80 mM NaCl at 25 °C) plotted as normalized fluorescence [$F_n = (F - F_0)/F_0$] *versus* ratio of total protein to DNA concentrations (where F_0 = fluorescence intensity of DNA alone and F is the fluorescence measured at each point in the titration). The biphasic nature of the *Ec*-SSB binding isotherm indicates formation of two types of complexes—the first having one tetramer [$(SSB)_{65}$ mode] and the second having two tetramers [$(SSB)_{35}$ mode] bound and characterized by high and low FRET values, respectively. The data fit to a model describing two sequential binding sites with $K_1 = 0.9 \times 10^{10}$ M^{-1} (minimum estimate) and $K_2 = 6.4 \times 10^7$ M^{-1}. For *Pf*-SSB, tight binding of the first tetramer with high FRET [$(SSB)_{65}$] is evident ($K_1 = > 1 \times 10^{10}$ M^{-1}; minimum estimate) but binding of the second tetramer [$(SSB)_{35}$] is extremely weak ($K_2 = 1 \times 10^6$ M^{-1}) and a very small decrease in FRET is observed.

We first compared titrations of *Pf*-SSB and *Ec*-SSB with $(dT)_{35}$ at low (10 mM NaCl; Fig. 4a) and moderate (200 mM NaCl; Fig. 4b) [NaCl] (buffer H, pH 8.1, 25 °C), monitoring the quenching of the intrinsic Trp fluorescence upon binding $(dT)_{35}$. At either [NaCl], *Pf*-SSB (filled squares) binds two molecules of $(dT)_{35}$ with high affinity (stoichiometrically) such that we were only able to estimate a lower limit for the binding affinities ($K_{1,obs}$, $K_{2,obs} > 10^{10}$ M^{-1}). On the other hand, whereas *Ec*-SSB tetramers (open circles) also bind the first $(dT)_{35}$ molecule stoichiometrically, the second $(dT)_{35}$ molecule binds with much weaker affinity in agreement with previous studies.[20] In addition, the affinity of *Ec*-SSB for the second $(dT)_{35}$ molecule decreases ~200-fold as the [NaCl] decreases from 0.2 M [$K_{2,obs} = (1.1 \pm 0.2) \times 10^8$ M^{-1}] to 10 mM [$K_{2,obs} = (5.1 \pm 0.4) \times 10^5$ M^{-1}] as observed previously.[20] Therefore, *Ec*-SSB tetramers show a dramatic salt-dependent negative cooperativity for binding a second $(dT)_{35}$ molecule, whereas *Pf*-SSB tetramers show no evidence for such negative cooperativity under these conditions. Due to the fact that both $(dT)_{35}$ molecules bind stoichiometrically to *Pf*-SSB under the conditions used in the fluorescence titrations discussed above, it is possible that some degree of negative cooperativity exists for the binding of the second molecule of $(dT)_{35}$, although if this occurs it is clearly not as extreme as for *Ec*-SSB.

Although we cannot determine the binding affinities of $(dT)_{35}$ for *Pf*-SSB under these tight binding conditions, we can measure the binding enthalpies using isothermal titration calorimetry (ITC).[26,28] The results of ITC experiments examining the binding of $(dT)_{35}$ to *Pf*-SSB (filled squares) and *Ec*-SSB (open circles) tetramers at 4 mM and 0.20 M NaCl (buffer H, pH 8.1, 25 °C) are shown in Fig. 4c and d, respectively. The biphasic nature of all titration isotherms in Fig. 4c and d indicates that both proteins can bind two molecules of $(dT)_{35}$ at saturation. As expected, *Ec*-SSB binds the first molecule of $(dT)_{35}$ stoichiometrically ($K_{1,obs} > 1 \times 10^{10}$ M^{-1}) at both low and moderate salt concentrations (see Fig. 4c and d, open circles); hence, only the binding enthalpies ($\Delta H_{1,obs} = -73.1 \pm 0.9$ kcal mol^{-1} at 4 mM NaCl and $\Delta H_{1,obs} = -66.6 \pm 0.5$ kcal mol^{-1} at 0.2 M NaCl) can be determined from the flat portions of the isotherms at $[(dT)_{35}]_{tot}/[\text{Ec-SSB}]_{tot} \leq 1$. However, we can estimate a binding affinity for the second molecule of $(dT)_{35}$ to *Ec*-SSB ($[(dT)_{35}]_{tot}/[\text{Ec-SSB}]_{tot} > 1$), which becomes much less favorable at low salt conditions with the affinity decreasing ~400-fold and binding enthalpy decreasing ~2-fold [$K_{2,obs} = (1.0 \pm 0.04) \times 10^8$ M^{-1} and $\Delta H_{2,obs} = -71.2 \pm 0.5$ kcal mol^{-1} at 0.2 M NaCl; $K_{2,obs} = (2.4 \pm 0.2) \times 10^5$ M^{-1} and $\Delta H_{2,obs} = -38.6 \pm 12$ kcal mol^{-1} at 4 mM NaCl], consistent with previous studies.[28]

Pf-SSB also binds the first molecule of $(dT)_{35}$ stoichiometrically and with similar enthalpies [$\Delta H_{1,obs} = -73.8 \pm 0.2$ kcal mol^{-1} at 4 mM NaCl and $\Delta H_{1,obs} = -70.9 \pm 0.2$ kcal mol^{-1} at 0.2 M NaCl

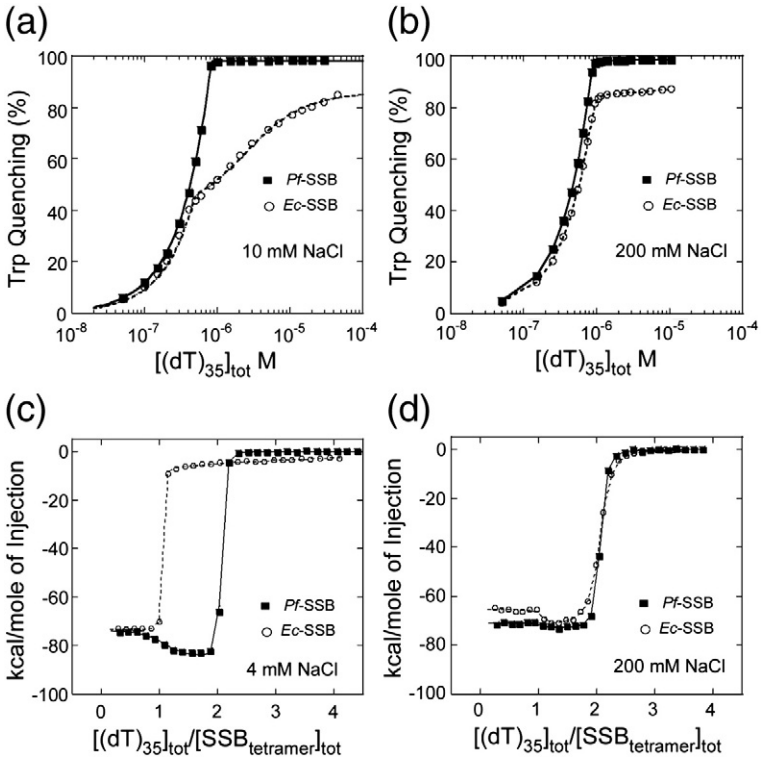

Fig. 4. *Pf*-SSB binds to two molecules of $(dT)_{35}$ with high affinity irrespective of the [NaCl] in solution. Fluorescence titrations showing binding to two $(dT)_{35}$ molecules to *Pf*-SSB or *Ec*-SSB at low NaCl [10 mM, (a)] and moderate NaCl [200 mM, (b)] conditions. *Pf*-SSB binds stoichiometrically to two molecules of $(dT)_{35}$ irrespective of [NaCl]. *Ec*-SSB binds stoichiometrically two $(dT)_{35}$ molecules at moderate [NaCl] but binds the second $(dT)_{35}$ molecule with significantly reduced affinity at low [NaCl] ($K_{2,obs} = 7.9 \pm 0.9 \times 10^5$ M^{-1}). Fits describing a sequential two-site binding model for *Pf*-SSB (continuous line) and *Ec*-SSB (dotted line) are also depicted. (c) Changes in enthalpy associated with binding of $(dT)_{35}$ to SSB in buffer H with 4 mM NaCl at 25 °C demonstrate sequential binding of two $(dT)_{35}$ molecules to *Ec*-SSB or *Pf*-SSB. For *Ec*-SSB, the first $(dT)_{35}$ molecule binds stoichiometrically ($\Delta H_{1,obs} = -73 \pm 0.01$ kcal mol^{-1}) and the second $(dT)_{35}$ molecule binds with weaker affinity ($K_2 = 2.43 \pm 0.2 \times 10^5$ M^{-1} and $\Delta H_{2,obs} = -38.6 \pm 0.25$ kcal mol^{-1}) and with negative cooperativity. For *Pf*-SSB, two $(dT)_{35}$ molecules bind stoichiometrically, yielding $\Delta H_{1,obs} = -73.7 \pm 0.2$ kcal mol^{-1} and $\Delta H_{2,obs} = -84.7 \pm 0.2$ kcal mol^{-1}, respectively, and almost no evidence of negative cooperativity. (d) Similar experiments done in buffer H with 200 mM NaCl yield stoichiometric binding of two $(dT)_{35}$ molecules to *Ec*-SSB ($\Delta H_{1,obs} = -65.4 \pm 0.2$ kcal mol^{-1} and $\Delta H_{2,obs} = -72 \pm 0.2$ kcal mol^{-1}, respectively). Under these conditions, *Pf*-SSB again binds two $(dT)_{35}$ stoichiometrically with observed heat changes of $\Delta H_{2,obs} = -73.4 \pm 0.2$ kcal mol^{-1} for binding of the first and second $(dT)_{35}$ molecules, respectively. At high salt conditions, there is no evidence of negative cooperativity for either SSB protein.

(see Fig. 4c and d, filled squares)] to those measured for *Ec*-SSB (see above). However, binding of the second $(dT)_{35}$ is strikingly different for *Pf*-SSB than for *Ec*-SSB. Whereas the apparent affinity of the second molecule of $(dT)_{35}$ decreases with decreasing [NaCl] for *Ec*-SSB, it increases with decreasing [NaCl] for *Pf*-SSB [$K_{2,obs} = (5.5 \pm 0.2) \times 10^8$ M^{-1} and $\Delta H_{2,obs} = -73.4 \pm 0.2$ kcal mol^{-1} at 0.2 M NaCl; $K_{2,obs} > 10^9$ M^{-1} and $\Delta H_{2,obs} = -84.8 \pm 0.3$ kcal mol^{-1} at 4 mM NaCl]. Therefore, not only do these experiments show no evidence for negative cooperativity in the *Pf*-SSB system, the dependence of $K_{2,obs}$ on [NaCl] is opposite for the two systems.

smFRET analysis show that *Pf*-SSB is capable of diffusion along ssDNA with transient melting of a DNA hairpin

Single-molecule FRET (smFRET) studies have demonstrated that *Ec*-SSB tetramers are able to diffuse along ssDNA and transiently melt a DNA hairpin.[10,11] This activity is responsible for the ability of SSB to remove secondary structures in DNA (such as hairpins) and facilitate RecA filament formation on ssDNA.[10] We therefore examined *Pf*-SSB tetramers using the same approach. In these experiments, we used an immobilized DNA substrate with an 18-bp double-stranded DNA handle and a 3′ 65-nt ssDNA extension followed by a 7-bp internal hairpin (as depicted in Fig. 5a).

Cy3 and Cy5 fluorophores are positioned at the stem of the hairpin as depicted in Fig. 5 such that the FRET value is sensitive to the formation or disruption of the hairpin.[10] When the hairpin is intact, the fluorophores are in close proximity, resulting in a high FRET state, whereas hairpin disruption results in a decrease in FRET.

The smFRET experiments were performed in the presence of 0.5 M NaCl, conditions under which both *Ec*-SSB and *Pf*-SSB tetramers bind ssDNA in a fully wrapped DNA binding mode and thus any changes in FRET are not due to fluctuations between SSB DNA binding modes but reflect opening/closing of the hairpin due to transient SSB disruption of the hairpin base pairs.[10,25] Furthermore, after addition of SSB protein, all free SSB protein was removed by flowing buffer (400 μl) over the surface. Hence, any FRET fluctuations in the presence of SSB

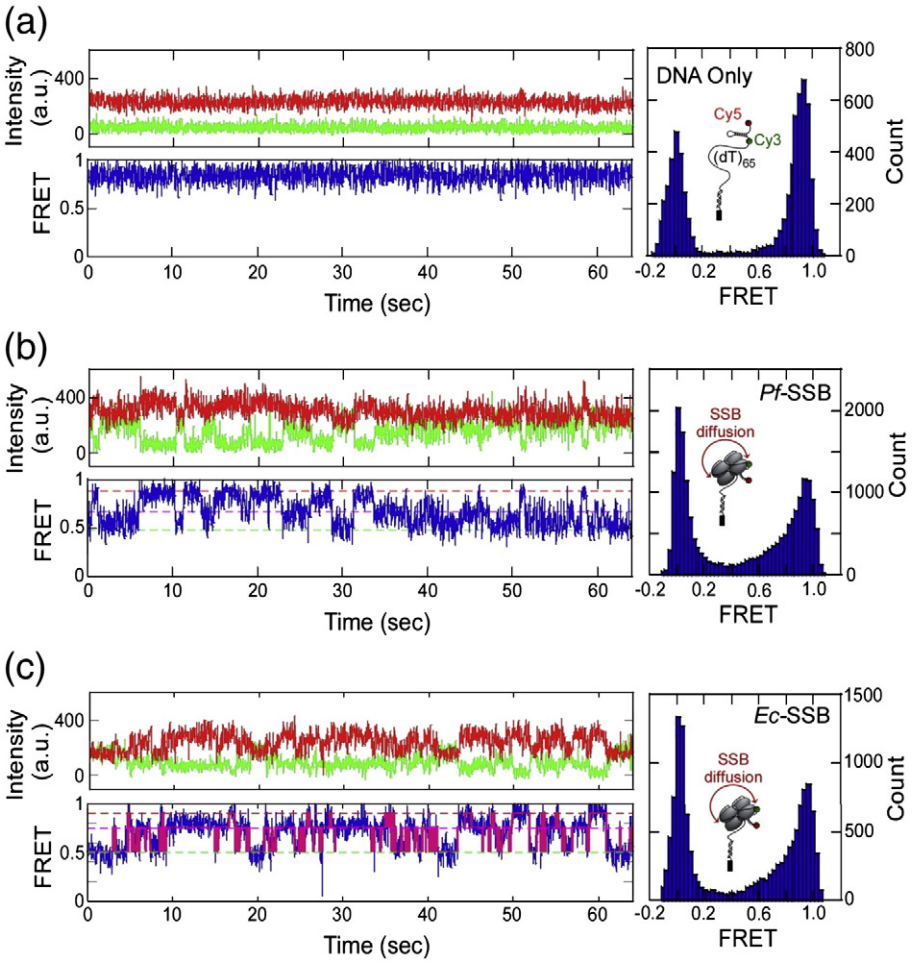

Fig. 5. smFRET analysis of SSB sliding on DNA. Time record of change in fluorescence of donor (Cy3, green trace) and acceptor (Cy5, red) and the resulting change in FRET (blue) are shown for a single DNA molecule in the absence of SSB (a) or in the presence of *Pf*-SSB (b) or *Ec*-SSB (c). The histograms representing the distribution of average FRET efficiency values for each experiment are also shown. The dotted lines represent the three transitions in FRET values observed when SSB diffuses along the ssDNA and unwinds the hairpin in the DNA. The DNA substrates used for these experiments are schematically depicted and the black rectangle denotes the glass surface onto which the double-stranded DNA handle is tethered. The pink trace in (c) represents an HMM analysis of the individual FRET states during the melting of the hairpin.

are due to SSB that is DNA bound. Figure 5a shows that in the absence of SSB, we observe a high FRET signal with few fluctuations, consistent with the formation of a stable hairpin in the DNA. The histogram of FRET efficiency compiled from multiple (~6000–8000) single DNA molecules shows a distinct peak with FRET efficiency ~0.90. The FRET efficiency peak near 0 reflects DNA molecules in which photobleaching of the Cy5 dye has occurred.[10,25] When *Pf*-SSB or *Ec*-SSB is flowed into the reaction chamber, SSB binds the DNA and we observe rapid fluctuations in the FRET efficiency (Fig. 5b and c). The distribution of molecules in various FRET states becomes much broader, ranging from 0.2 to 1.0. This suggests that the base pairs within the hairpin become melted transiently by the SSB proteins. As previously reported, this reflects SSB diffusion along the ssDNA and transient melting of the hairpin.[10,25] Analysis of the individual traces shows the presence of three distinct DNA states (dotted lines in Fig. 5) during the SSB diffusion process.

Although both *Ec*-SSB and *Pf*-SSB show the same ability to diffuse along ssDNA and transiently melt a hairpin DNA, there are clear differences in the smFRET fluctuation patterns observed for each protein. Hidden Markov model (HMM) analysis of the individual traces reveals differences in the transitions among the three FRET states (Fig. 5c). In the case of *Ec*-SSB, these transitions are rapid and distinct and are well defined by HMM analysis. However, for *Pf*-SSB, the transitions are not as sharp

(Fig. 5b) and hence are not suitable for HMM analysis. This suggests differences in their mechanisms of diffusion and/or transient DNA melting.

Discussion

Ec-SSB can bind to single-stranded poly(dT) in two fully wrapped modes, referred to as the $(SSB)_{55}$ and $(SSB)_{65}$ binding modes, as well as a partially wrapped, highly cooperative $(SSB)_{35}$ binding mode. The transitions among these binding modes are salt and protein binding density dependent, and it has been proposed that the different modes function in different DNA metabolic events such as replication, repair, and recombination.[9] The ability to bind ssDNA in multiple modes has also been observed for other SSBs such as yeast RPA[29] and the *Deinococcus radiodurans*[30] and *Thermus aquaticus* SSBs.[31] Surprisingly, we show here that *Pf*-SSB tetramers bind single-stranded poly(dT) only in the fully wrapped modes *in vitro* with occluded site size between 55 and 62 nt (Figs. 1 and 2), with no evidence for a lower site size, highly cooperative ssDNA binding mode. Just as *Ec*-SSB shows a high salt transition between an $(SSB)_{55}$ and an $(SSB)_{65}$ binding mode on poly(dT), *Pf*-SSB shows a similar transition between an $(SSB)_{55}$ and $(SSB)_{62}$ binding mode. Based on their crystal structures, we predict that in both of these modes, all four subunits interact with the ssDNA (Fig. 6). The different SSB binding modes make different amounts of DNA accessible to other proteins. It has been proposed that the lower site size, highly cooperative $(SSB)_{35}$ DNA binding mode observed for *Ec*-SSB is involved in DNA replication, although this has not been demonstrated.[7,16] If *Pf*-SSB is involved in DNA replication of the apicoplast genome, the absence of this binding mode for *Pf*-SSB *in vitro* may suggest that such a highly cooperative binding mode is not essential. However, it is also possible that *Pf*-SSB interacts with a completely different set of auxiliary proteins that facilitate *Pf*-SSB to adopt alternate binding modes on the DNA during apicoplast DNA replication/maintenance.

Both the *Ec*-SSB[10,11] and *Pf*-SSB tetramers are able to diffuse along ssDNA and transiently melt out a DNA hairpin while bound in their fully wrapped modes. The ability of *Ec*-SSB to slide on DNA and remove secondary structures such as hairpins has been shown to facilitate the formation of RecA filaments on natural ssDNA.[10] Thus, the ability of *Pf*-SSB to diffuse along ssDNA and remove secondary structures in the DNA might also be functionally important for apicoplast DNA maintenance. Although *P. falciparum* also contains a Rad51 protein (a homolog of RecA), it is not known whether this protein localizes to the apicoplast.[32]

Origins of the $(SSB)_{35}$ binding mode

The ability of *Ec*-SSB tetramers to bind ssDNA in multiple binding modes *in vitro* has been known for over 25 years,[15,18] although the molecular bases for the stability of each mode as well as the functional importance of each mode *in vivo* are not well understood. The high degree of structural and sequence conservation between *Ec*-SSB and *Pf*-SSB in combination with the absence of the $(SSB)_{35}$ DNA binding mode for *Pf*-SSB may provide an opportunity to probe the structural basis for the $(SSB)_{35}$ mode of *Ec*-SSB. In the *Ec*-SSB tetramer, under low salt conditions where the $(SSB)_{35}$ binding mode is favored, a strong negative

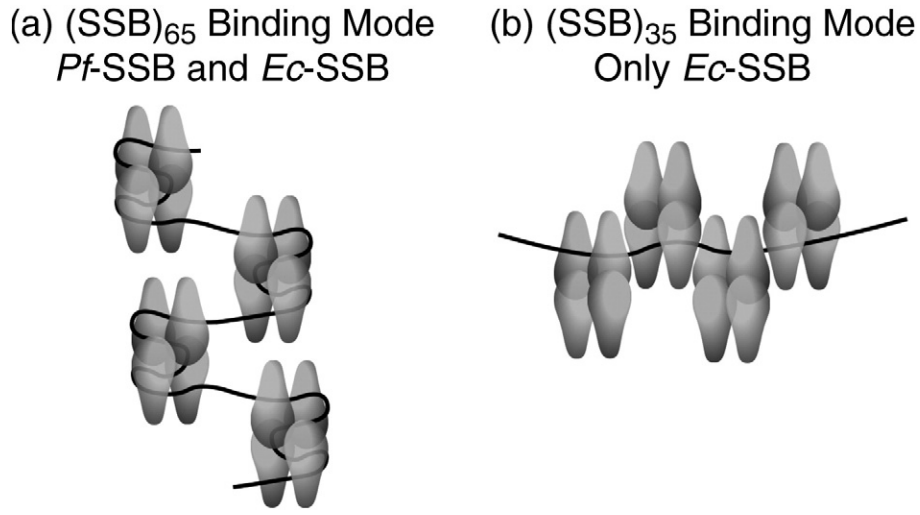

Fig. 6. Models for DNA binding. (a) *Pf*-SSB and *Ec*-SSB can adopt the $(SSB)_{65}$ DNA binding mode, but (b) only *Ec*-SSB possesses the cooperative $(SSB)_{35}$ DNA binding mode.

cooperativity is observed for ssDNA binding to the third and fourth subunits of the tetramer (Fig. 4). Although the molecular basis for this negative cooperativity is not well understood, this property is severely reduced or even nonexistent in *Pf*-SSB, which is one reason that only the fully wrapped DNA binding mode is observed (Fig. 6). As described in an accompanying article (E.A. *et al.*), there are a number of structural differences between these two proteins that might explain the difference in DNA binding properties: (a) the ssDNA is wrapped around each tetramer with opposite polarities; (b) asymmetric protein–DNA contacts are observed among the *Ec*-SSB subunits, but not *Pf*-SSB subunits; (c) different inter-tetramer contacts are observed in the crystal structures.

In the *Pf*-SSB–ssDNA complex, the DNA wraps around the protein with opposite backbone polarity compared to the *Ec*-SSB–ssDNA structure, such that the ssDNA wrapping topologies are mirror images of each other (E.A. *et al.*, accompanying article). In addition, the protein–DNA contacts are the same within the four subunits in *Pf*-SSB but show asymmetries among the *Ec*-SSB subunits. This asymmetry might reflect the ability of the individual monomers within the *Ec*-SSB tetramer to interact differently with the DNA and thereby enable formation of the $(SSB)_{35}$ binding mode. The absence of these asymmetric contacts may favor a fully wrapped DNA binding mode for *Pf*-SSB.

A fourth possibility is that the unstructured C-termini of SSB contributes to the observed differences in DNA binding modes. The C-terminal tails of the *Ec*-SSB tetramer have been shown to regulate its DNA binding activity[33] *in vitro*, and deletion of the tail shifts the $(SSB)_{35}$ to $(SSB)_{65}$ equilibrium to favor the $(SSB)_{35}$ mode.[25] Since the C-terminus of *Pf*-SSB is different in sequence composition, it remains to be seen whether it displays the same effects as observed with *Ec*-SSB. The mitochondrial SSB protein (mtSSB) from higher eukaryotes is also homotetrameric[34] and highly homologous to the DNA binding core of *Ec*- and *Pf*-SSB[35] but does not possess the unstructured C-terminal tails.[36] The human mtSSB has been shown to bind ssDNA with a site size of about 50–70 nt at moderate to high [NaCl];[35] however, whether it can form a cooperative $(SSB)_{35}$ mode at lower [NaCl] has not been examined. The precise function of mtSSB is not known, but even though it does not possess disordered C-terminal tails, it still physically interacts with other proteins such as p53[37] and functions in the replication and maintenance of the mitochondrial DNA. The differences in the DNA binding properties of *Pf*-SSB along with the unique composition of its C-terminal tails highlight possible divergent roles in the *Plasmodium* parasite and make it a potentially ideal target for antimalarial drug development.

Materials and Methods

Buffers

All experiments were performed in Buffer Hx containing 10 mM Hepes, pH 8.1, 1 mM EDTA (ethylenediaminetetraacetic acid), and 1 mM tris(2-carboxyethyl) phosphine, where "X" denotes the molar concentration of NaCl. Binding buffer used in the smFRET experiments is 10 mM Tris, pH 8.1, and 50 mM NaCl. Imaging buffer[38] is 10 mM Tris, pH 8.1, 0.1 mM Na2EDTA, 0.1 mg/ml bovine serum albumin, 1 mM DTT, 1% Dextrose, 3 mM Trolox (6-hydroxy-2,5,7,8-tetramethylchroman-2-carboxylic acid, Sigma Aldrich, Missouri), 0.1 mg/ml glucose oxidase (Type VII, from *Aspergillus*, Sigma Aldrich), 0.004 mg/ml catalase (from bovine liver, Sigma Aldrich), with 500 mM NaCl.

Proteins and DNA

Pf-SSB and *Ec*-SSB proteins were expressed and purified as described (E.A. *et al.*, accompanying article) and their concentrations were determined using the following extinction coefficients: $\varepsilon_{260} = 1.13 \times 105\ M^{-1}\ cm^{-1}$ (*Ec*-SSB tetramer[15]) and $\varepsilon_{260} = 9.58 \times 104\ M^{-1}\ cm^{-1}$ (*Pf*-SSB tetramer) (E.A. *et al.*, accompanying article).

The oligodeoxynucleotides, $(dT)_{35}$ and 5′-Cy5-dT_{68}-Cy3-dT were synthesized and purified as previously described.[39] Poly(dT) was purchased from Midland Certified Reagent Co. (Midland, TX) and dialyzed extensively against buffer (3500 Da molecular mass cutoff) (Spectrum Inc., Houston, TX). Phage M13mp18 ssDNA was purchased from New England Biolabs (Ipswich, MA). All ssDNA concentrations were determined spectrophotometrically using the extinction coefficient $\varepsilon_{260} = 8.1 \times 10^3\ M^{-1}$ (nucleotide) cm^{-1} for oligo(dT) and poly(dT)[40] and an $\varepsilon_{259} = 7370\ M^{-1}\ cm^{-1}$ for ssM13 DNA in buffer $H^{0.02}$.[41] The concentration of 5′-Cy5-dT_{68}-Cy3-dT was determined by measuring its absorbance using the extinction coefficient $\varepsilon_{260} = 5.74 \times 10^5\ M^{-1}\ cm^{-1}$.[24]

For the smFRET experiments, the short biotinylated DNA strand (5′-GCCTCGCTGCCGTCGCCA-biotin-3′) was annealed with the longer DNA strand containing Cy3 and Cy5 dyes [5′-TGGCGACGGCAGCGAGGC-$(T)_{65}$-Cy3-TGTGACTGAGACAGTCACTT-Cy5-T-3′] in 10 mM Tris (pH 8.1) and 0.1 M NaCl. The longer DNA strand contains three segments: the 5′ 18 nt are complementary to the short DNA, a stretch of $(dT)_{65}$, and a hairpin containing Cy3 (donor) and Cy5 (acceptor) towards the 3′-end. The DNA strands were annealed by mixing 11 μM non-biotin strand and 10 μM biotin strand, heating the sample to 95 °C for 2 min, and allowing the sample to slowly cool to room temperature.

Fluorescence titrations

Binding of *Pf*-SSB or *Ec*-SSB to poly(dT) and $(dT)_{35}$ was examined by monitoring the quenching of intrinsic protein tryptophan fluorescence upon titration with DNA (PTI-QM-2000 spectrofluorometer, PTI Inc., Lawrenceville, NJ) [$\lambda_{ex} = 296$ nm (2 nm band-pass), and $\lambda_{em} = 345$ nm (2–5 nm band-pass)] with corrections

applied as previously described.[42,43] Changes in Cy5 fluorescence upon binding two molecules of either *Pf*-SSB or *Ec*-SSB to a 5′-Cy5-$(dT)_{68}$-Cy3-dT DNA were examined by exciting the Cy3 donor at 515 nm and monitoring sensitized emission from the Cy5 acceptor at 664 nm (Fig. 3b). The titration data were fit to the sequential two-site binding model described in Eq. (1a):

$$F_{\text{obs}} = \frac{F_1 K_{1,\text{obs}} P + F_2 K_{1,\text{obs}} K_{2,\text{obs}} P^2}{1 + K_{1,\text{obs}} P + K_{1,\text{obs}} K_{2,\text{obs}} P^2} \tag{1a}$$

where $F_{\text{obs}} = (F_i - F_0)/F_0$ is the observed change (enhancement) in Cy5 fluorescence normalized to the Cy5 fluorescence of free DNA (F_0), F_1 is the change in Cy5 signal upon binding of the first tetramer to the ssDNA, and F_2 is the change in Cy5 signal upon binding two tetramers to the ssDNA. $K_{1,\text{obs}}$ and $K_{2,\text{obs}}$ are the stepwise macroscopic association equilibrium constants for the binding of the first and second SSB tetramer, respectively ($K_{1,\text{obs}} = [\text{PD}]/[\text{P}][\text{D}]$ and $K_{2,\text{obs}} = [\text{P2D}]/[\text{PD}][\text{P}]$) (i.e., statistical factors are not considered explicitly). The concentration of free SSB tetramer, P, was determined from mass conservation as in Eq. (1b):

$$P_{\text{tot}} = P + \frac{K_{1,\text{obs}} P + 2K_{1,\text{obs}} K_{2,\text{obs}} P^2}{1 + K_{1,\text{obs}} P + K_{1,\text{obs}} K_{2,\text{obs}} P^2} D_{\text{tot}} \tag{1b}$$

Data fitting was performed using the program SCIENTIST (Micromath Research, St. Louis, MO).

The same model was used to describe binding of two $(dT)_{35}$ molecules to either *Ec*-SSB or *Pf*-SSB tetramers (Fig. 4a and b). In this case, the protein (P) is considered as a macromolecule and $(dT)_{35}$ (D) is considered as a ligand and, therefore, Eqs. (1a) and (1b) should be rewritten in the form of Eqs. (2a) and (2b)

$$Q_{\text{obs}} = \frac{Q_1 K_{1,\text{obs}} D + Q_2 K_{1,\text{obs}} K_{2,\text{obs}} D^2}{1 + K_{1,\text{obs}} D + K_{1,\text{obs}} K_{2,\text{obs}} D^2} \tag{2a}$$

$$D_{\text{tot}} = D + \frac{K_{1,\text{obs}} D + 2K_{1,\text{obs}} K_{2,\text{obs}} D^2}{1 + K_{1,\text{obs}} D + K_{1,\text{obs}} K_{2,\text{obs}} D^2} P_{\text{tot}} \tag{2b}$$

where $Q_{\text{obs}} = (F_0 - F_i)/F_0$ is the observed change (quenching) of intrinsic Trp fluorescence of the protein upon DNA binding normalized to the fluorescence of free protein (F_0), and binding parameters Q_1, Q_2, $K_{1,\text{obs}}$, and $K_{2,\text{obs}}$ are defined as above for the binding of the first and the second molecule of $(dT)_{35}$ to SSB tetramer.

Negative staining and analysis by electron microscopy

Pf-SSB or *Ec*-SSB (291 nM) was mixed with M13mp18 ssDNA (1 nM nucleotides) in buffer H (with either 4 or 200 mM NaCl) at 22 °C in 50 μl total volume. A 1.5-fold molar excess of SSB tetramer over DNA sites was used assuming a binding site size of 33 nt/tetramer at saturation.[14] Samples (20 μl) were fixed with 1% glutaraldehyde (Polysciences Inc., Warrington, PA) for 10 min and subsequently adsorbed onto glow-discharged formvar/carbon-coated copper grids for 10 min. Grids were washed in ddH_2O and stained with 1% aqueous uranyl acetate (Ted Pella Inc., Redding CA) for 1 min.

Excess liquid was gently wicked off and grids were allowed to air dry. Samples were viewed on a JEOL 1200EX transmission electron microscope (JEOL USA, Peabody, MA) at an accelerating voltage of 80 kV.

Isothermal titration calorimetry

ITC experiments were performed using a VP-ITC microcalorimeter (GE Inc., Piscataway, NJ) by titrating *Pf*-SSB or *Ec*-SSB solutions in the cell (1 μM tetramer) with $(dT)_{35}$ (15–24 μM concentrations in the syringe) in buffer H with NaCl concentrations as noted in each experiment. The reference heats of dilutions were determined by titrating DNA solution into the buffer in the cell. Both protein and DNA solutions were dialyzed extensively against the buffer prior to each experiment. The ITC data for SSB tetramer binding to two molecules of $(dT)_{35}$ were analyzed as previously described[28] using a two-site sequential binding model characterized by two macroscopic stepwise binding constants ($K_{1,\text{obs}}$ and $K_{2,\text{obs}}$) and two binding enthalpies ($\Delta H_{1,\text{obs}}$ and $\Delta H_{2,\text{obs}}$), such that the total heat (Q_i^{tot}) after the ith injection is defined by Eq. (3):

$$Q_i^{\text{tot}} = V_0 \cdot P_{\text{tot}} \times \left(\frac{K_{1,\text{obs}} D \cdot \Delta H_{1,\text{obs}} + K_{1,\text{obs}} K_{2,\text{obs}} D^2 \left(\Delta H_{2,\text{obs}} \right)}{1 + K_{1,\text{obs}} D + K_{1,\text{obs}} K_{2,\text{obs}} D^2} \right) \tag{3}$$

where the concentration of free DNA (D) is obtained by solving Eq. (2b), in which D_{tot} and P_{tot} are the total concentrations of the DNA and SSB, respectively, in the calorimetric cell after the ith injection. The conversion of integral heats (Q_i^{tot}) to differential heats (heats per injection observed in the experiment) and the nonlinear least squares fitting of the data were performed as previously described.[28]

smFRET experiments

smFRET experiments were performed as previously described.[10,25] A two-channel flow assembly was prepared as previously described[44,45] and both channels were coated with a freshly prepared solution containing 1.5% (w/v) biotin-polyethylene glycol-succinimidyl valerate (average molecular weight, 5000) and 25% (w/v) methoxy polyethylene glycol-succinimidyl valerate (average molecular weight, 5000) (Laysan Bio, Arab, AL) in 0.1 M $NaHCO_3$ (pH 8.1) for at least 3 h.[46] The flow channels were washed with water and, if needed, were subjected to photobleaching by a high-intensity laser (532 nm) to remove background signals. A 0.2 mg/ml solution of NeutrAvidin (Thermo Scientific, Massachusetts) in binding buffer was flowed into the channels and incubated for 5 min and excess NeutrAvidin was washed away. DNA was attached to the slide, by flowing 10 pM of biotinylated DNA over the surface followed by incubation for 5–10 min. Free DNA was washed away with 200 μl of binding buffer and the channel was filled with imaging buffer.

Single-molecule total internal reflectance fluorescence experiments were performed with an objective-type total internal reflection microscope (Olympus IX71, model IX2_MPITIRTL) equipped with a three-laser system (488 nm, 532 nm, and 635 nm) and an oil-immersed, high numerical aperture TIRFM objective (PlanApo N,

60×/1.45 N.A., Olympus). Fluorescence of the Cy3 dye on the DNA was excited with a 532-nm laser reflecting through a dichroic mirror (Z532RDC), and its fluorescence emission was passed through the dichroic mirror and a 550-nm long-pass filter (HQ550LP). Donor (Cy3) and acceptor (Cy5) emission intensities were separated with a split imaging TV port (U-SIP) consisting of a dichroic mirror (T640LPXR) and two additional band-pass filters. The short-wavelength (Cy3) signal was passed through a 585-nm band-pass filter (ET585/65M), and the long-wavelength (Cy5) signal was passed through a 700- nm band-pass filter (ET700/75M) and captured by a CCD camera (iXonEM+ DU-897E-CSO-#BV, Andor Technology, Connecticut). The donor and acceptor images were overlaid by adjusting mirrors in the split image unit using crimson fluorescent microspheres (0.2 μm, 2% solid, diluted 1000×, Invitrogen, California) as a reference image. Intense fluorescent signals appear on both channels, allowing unambiguous alignment of the two images. The image was further aligned using a mapping algorithm in the data collection and analysis packages kindly supplied by T. Ha (University of Illinois‡). Experiments were performed at 23 °C in imaging buffer. Typically, 2000 frames were recorded (within 64 s) with a 30-ms integration time at every spot (20 to 50 spots). Data acquisition and analyses were performed as previously described.[10,25] Correction for leakages and instrument detection efficiencies were performed on the FRET signal.[25,44,47] We observed ~12% leakage of donor onto the acceptor channel (measured using a DNA labeled only with Cy3). The detection efficiency was calculated using the ratio of acceptor intensity change to donor intensity change ($\Delta I_a/\Delta I_d$) at the acceptor photobleached event as previously described.[47] With 39 acceptor photobleached events, the distribution of $\Delta I_a/\Delta I_d$ had a median value of 0.93. HMM analysis was applied to the FRET traces where discrete changes were observed using methods previously described.[48]

Supplementary data related to this article can be found online at doi:10.1016/j.jmb.2012.04.022

Acknowledgements

We thank Thang Ho for synthesis and purification of the oligodeoxynucleotides, Dr. Wandy Beatty for assistance with the electron microscopy experiments, and Dr. R. Galletto for help with the smFRET instrument and experiments and Dr. Taekjip Ha for providing advice and software for the smFRET analysis. This work was supported in part by grants from the National Institutes of Health (GM30498 and GM45948) to T.M.L.

References

1. Snow, R. W., Guerra, C. A., Noor, A. M., Myint, H. Y. & Hay, S. I. (2005). The global distribution of clinical episodes of *Plasmodium falciparum* malaria. *Nature*, **434**, 214–217.
2. Wilson, R. J., Denny, P. W., Preiser, P. R., Rangachari, K., Roberts, K., Roy, A. *et al.* (1996). Complete gene map of the plastid-like DNA of the malaria parasite *Plasmodium falciparum*. *J. Mol. Biol.* **261**, 155–172.
3. Dahl, E. L. & Rosenthal, P. J. (2008). Apicoplast translation, transcription and genome replication: targets for antimalarial antibiotics. *Trends Parasitol.* **24**, 279–284.
4. Prusty, D., Dar, A., Priya, R., Sharma, A., Dana, S., Choudhury, N. R. *et al.* (2010). Single-stranded DNA binding protein from human malarial parasite *Plasmodium falciparum* is encoded in the nucleus and targeted to the apicoplast. *Nucleic Acids Res.* **38**, 7037–7053.
5. Lu, D., Bernstein, D. A., Satyshur, K. A. & Keck, J. L. (2010). Small-molecule tools for dissecting the roles of SSB/protein interactions in genome maintenance. *Proc. Natl Acad. Sci. USA*, **107**, 633–638.
6. Lu, D., Windsor, M. A., Gellman, S. H. & Keck, J. L. (2009). Peptide inhibitors identify roles for SSB C-terminal residues in SSB/exonuclease I complex formation. *Biochemistry*, **48**, 6764–6771.
7. Lohman, T. M., Bujalowski, W. & Overman, L. B. (1988). *E. coli* single strand binding protein: a new look at helix-destabilizing proteins. *Trends Biochem. Sci.* **13**, 250–255.
8. Shereda, R. D., Kozlov, A. G., Lohman, T. M., Cox, M. M. & Keck, J. L. (2008). SSB as an organizer/mobilizer of genome maintenance complexes. *Crit. Rev. Biochem. Mol. Biol.* **43**, 289–318.
9. Lohman, T. M. & Ferrari, M. E. (1994). *Escherichia coli* single-stranded DNA-binding protein: multiple DNA-binding modes and cooperativities. *Annu. Rev. Biochem.* **63**, 527–570.
10. Roy, R., Kozlov, A. G., Lohman, T. M. & Ha, T. (2009). SSB protein diffusion on single-stranded DNA stimulates RecA filament formation. *Nature*, **461**, 1092–1097.
11. Zhou, R., Kozlov, A. G., Roy, R., Zhang, J., Korolev, S., Lohman, T. M. & Ha, T. (2011). SSB functions as a sliding platform that migrates on DNA via reptation. *Cell*, **146**, 222–232.
12. Meyer, R. R. & Laine, P. S. (1990). The single-stranded DNA-binding protein of *Escherichia coli*. *Microbiol. Rev.* **54**, 342–380.
13. Bujalowski, W. & Lohman, T. M. (1986). *Escherichia coli* single-strand binding protein forms multiple, distinct complexes with single-stranded DNA. *Biochemistry*, **25**, 7799–7802.
14. Chrysogelos, S. & Griffith, J. (1982). *Escherichia coli* single-strand binding protein organizes single-stranded DNA in nucleosome-like units. *Proc. Natl Acad. Sci. USA*, **79**, 5803–5807.
15. Lohman, T. M. & Overman, L. B. (1985). Two binding modes in *Escherichia coli* single strand binding protein–single stranded DNA complexes. Modulation by NaCl concentration. *J. Biol. Chem.* **260**, 3594–3603.
16. Lohman, T. M., Overman, L. B. & Datta, S. (1986). Salt-dependent changes in the DNA binding co-operativity of *Escherichia coli* single strand binding protein. *J. Mol. Biol.* **187**, 603–615.
17. Bujalowski, W., Overman, L. B. & Lohman, T. M. (1988). Binding mode transitions of *Escherichia coli* single strand binding protein-single-stranded DNA complexes. Cation, anion, pH, and binding density effects. *J. Biol. Chem.* **263**, 4629–4640.

‡ https://physics.illinois.edu/cplc/software/

18. Griffith, J. D., Harris, L. D. & Register, J., III (1984). Visualization of SSB–ssDNA complexes active in the assembly of stable RecA-DNA filaments. *Cold Spring Harbor Symp. Quant. Biol.* **49**, 553–559.
19. Raghunathan, S., Kozlov, A. G., Lohman, T. M. & Waksman, G. (2000). Structure of the DNA binding domain of *E. coli* SSB bound to ssDNA. *Nat. Struct. Biol.* **7**, 648–652.
20. Bujalowski, W. & Lohman, T. M. (1989). Negative co-operativity in *Escherichia coli* single strand binding protein–oligonucleotide interactions. II. Salt, temperature and oligonucleotide length effects. *J. Mol. Biol.* **207**, 269–288.
21. Bujalowski, W. & Lohman, T. M. (1989). Negative co-operativity in *Escherichia coli* single strand binding protein-oligonucleotide interactions. I. Evidence and a quantitative model. *J. Mol. Biol.* **207**, 249–268.
22. Lohman, T. M. & Bujalowski, W. (1988). Negative cooperativity within individual tetramers of *Escherichia coli* single strand binding protein is responsible for the transition between the $(SSB)_{35}$ and (SSB)56 DNA binding modes. *Biochemistry*, **27**, 2260–2265.
23. McGhee, J. D. & von Hippel, P. H. (1974). Theoretical aspects of DNA–protein interactions: co-operative and non-co-operative binding of large ligands to a one-dimensional homogeneous lattice. *J. Mol. Biol.* **86**, 469–489.
24. Kozlov, A. G. & Lohman, T. M. (2002). Stopped-flow studies of the kinetics of single-stranded DNA binding and wrapping around the *Escherichia coli* SSB tetramer. *Biochemistry*, **41**, 6032–6044.
25. Roy, R., Kozlov, A. G., Lohman, T. M. & Ha, T. (2007). Dynamic structural rearrangements between DNA binding modes of *E. coli* SSB protein. *J. Mol. Biol.* **369**, 1244–1257.
26. Kozlov, A. G. & Lohman, T. M. (2011). *E. coli* SSB tetramer binds the first and second molecules of (dT)(35) with heat capacities of opposite sign. *Biophys. Chem.* **159**, 48–57.
27. Kozlov, A. G. & Lohman, T. M. (2006). Effects of monovalent anions on a temperature-dependent heat capacity change for *Escherichia coli* SSB tetramer binding to single-stranded DNA. *Biochemistry*, **45**, 5190–5205.
28. Kozlov, A. G. & Lohman, T. M. (1998). Calorimetric studies of *E. coli* SSB protein–single-stranded DNA interactions. Effects of monovalent salts on binding enthalpy. *J. Mol. Biol.* **278**, 999–1014.
29. Kumaran, S., Kozlov, A. G. & Lohman, T. M. (2006). *Saccharomyces cerevisiae* replication protein A binds to single-stranded DNA in multiple salt-dependent modes. *Biochemistry*, **45**, 11958–11973.
30. Kozlov, A. G., Eggington, J. M., Cox, M. M. & Lohman, T. M. (2010). Binding of the dimeric *Deinococcus radiodurans* single-stranded DNA binding protein to single-stranded DNA. *Biochemistry*, **49**, 8266–8275.
31. Witte, G., Fedorov, R. & Curth, U. (2008). Biophysical analysis of *Thermus aquaticus* single-stranded DNA binding protein. *Biophys. J.* **94**, 2269–2279.
32. Bhattacharyya, M. K. & Kumar, N. (2003). Identification and molecular characterisation of DNA damaging agent induced expression of *Plasmodium falciparum* recombination protein PfRad51. *Int. J. Parasitol.* **33**, 1385–1392.
33. Kozlov, A. G., Cox, M. M. & Lohman, T. M. (2010). Regulation of single-stranded DNA binding by the C termini of *Escherichia coli* single-stranded DNA-binding (SSB) protein. *J. Biol. Chem.* **285**, 17246–17252.
34. Li, K. & Williams, R. S. (1997). Tetramerization and single-stranded DNA binding properties of native and mutated forms of murine mitochondrial single-stranded DNA-binding proteins. *J. Biol. Chem.* **272**, 8686–8694.
35. Curth, U., Urbanke, C., Greipel, J., Gerberding, H., Tiranti, V. & Zeviani, M. (1994). Single-stranded-DNA-binding proteins from human mitochondria and *Escherichia coli* have analogous physicochemical properties. *Eur. J. Biochem.* **221**, 435–443.
36. Tiranti, V., Rocchi, M., DiDonato, S. & Zeviani, M. (1993). Cloning of human and rat cDNAs encoding the mitochondrial single-stranded DNA-binding protein (SSB). *Gene*, **126**, 219–225.
37. Wong, T. S., Rajagopalan, S., Townsley, F. M., Freund, S. M., Petrovich, M., Loakes, D. & Fersht, A. R. (2009). Physical and functional interactions between human mitochondrial single-stranded DNA-binding protein and tumour suppressor p53. *Nucleic Acids Res.* **37**, 568–581.
38. Rasnik, I., McKinney, S. A. & Ha, T. (2006). Non-blinking and long-lasting single-molecule fluorescence imaging. *Nat. Methods*, **3**, 891–893.
39. Ferrari, M. E., Bujalowski, W. & Lohman, T. M. (1994). Co-operative binding of *Escherichia coli* SSB tetramers to single-stranded DNA in the $(SSB)_{35}$ binding mode. *J. Mol. Biol.* **236**, 106–123.
40. Kowalczykowski, S. C., Lonberg, N., Newport, J. W. & von Hippel, P. H. (1981). Interactions of bacteriophage T4-coded gene 32 protein with nucleic acids. I. Characterization of the binding interactions. *J. Mol. Biol.* **145**, 75–104.
41. Berkowitz, S. A. & Day, L. A. (1974). Molecular weight of single-stranded fd bacteriophage DNA. High speed equilibrium sedimentation and light scattering measurements. *Biochemistry*, **13**, 4825–4831.
42. Ferrari, M. E. & Lohman, T. M. (1994). Apparent heat capacity change accompanying a nonspecific protein–DNA interaction. *Escherichia coli* SSB tetramer binding to oligodeoxyadenylates. *Biochemistry*, **33**, 12896–12910.
43. Lohman, T. M. & Mascotti, D. P. (1992). Nonspecific ligand–DNA equilibrium binding parameters determined by fluorescence methods. *Methods Enzymol.* **212**, 424–458.
44. Selvin, P. R. & Ha, T. (2008). *Single-Molecule Techniques: A Laboratory Manual.* Cold Spring Harbor Laboratory Press, Cold Spring Harbor, NY.
45. Selvin, P. R. (2011). *Methods in Molecular Biology—Single Molecule Enzymology: Methods and Protocols.* Humana Press, New York, NY.
46. Fili, N., Mashanov, G. I., Toseland, C. P., Batters, C., Wallace, M. I., Yeeles, J. T. *et al.* (2010). Visualizing helicases unwinding DNA at the single molecule level. *Nucleic Acids Res.* **38**, 4448–4457.
47. Ha, T., Ting, A. Y., Liang, J., Caldwell, W. B., Deniz, A. A., Chemla, D. S. *et al.* (1999). Single-molecule fluorescence spectroscopy of enzyme conformational dynamics and cleavage mechanism. *Proc. Natl Acad. Sci. USA*, **96**, 893–898.
48. McKinney, S. A., Joo, C. & Ha, T. (2006). Analysis of single-molecule FRET trajectories using hidden Markov modeling. *Biophys. J.* **91**, 1941–1951.